



HAL
open science

On the role of thermal boundary conditions in dynamo scaling laws

Ludivine Oruba

► **To cite this version:**

Ludivine Oruba. On the role of thermal boundary conditions in dynamo scaling laws. *Geophysical and Astrophysical Fluid Dynamics*, 2016, 110 (6), pp.529-545. 10.1080/03091929.2016.1217523 . insu-02471388

HAL Id: insu-02471388

<https://insu.hal.science/insu-02471388>

Submitted on 28 Nov 2022

HAL is a multi-disciplinary open access archive for the deposit and dissemination of scientific research documents, whether they are published or not. The documents may come from teaching and research institutions in France or abroad, or from public or private research centers.

L'archive ouverte pluridisciplinaire **HAL**, est destinée au dépôt et à la diffusion de documents scientifiques de niveau recherche, publiés ou non, émanant des établissements d'enseignement et de recherche français ou étrangers, des laboratoires publics ou privés.

On the role of thermal boundary conditions in dynamo scaling laws

Ludivine Oruba *

Physics Department, Ecole Normale Supérieure, 24 rue Lhomond, 75005 Paris, France

(Received 00 Month 20xx; final version received 00 Month 20xx)

In dynamo power-based scaling laws, the power P injected by buoyancy forces is measured by a so-called flux-based Rayleigh number, denoted as Ra_Q^* (see Christensen and Aubert, *Geophys. J. Int.* 2006, vol. 166, pp. 97-114). Whereas it is widely accepted that this parameter is measured (as opposite to controlled) in dynamos driven by differential heating, the literature is much less clear concerning its nature in the case of imposed heat flux. We clarify this issue by highlighting that in that case, the Ra_Q^* parameter becomes controlled only in the limit of large Nusselt numbers ($Nu \gg 1$).

We then address the issue of the robustness of the original relation between P and Ra_Q^* with the geometry and the thermal boundary conditions. We show that in the cartesian geometry, as in the spherical geometry with a central mass distribution, this relation is purely linear, in both differential and fixed-flux heating. However, we show that in the geometry commonly studied by geophysicists (spherical with uniform mass distribution), its validity places an upper-bound on the strength of the driving which can be envisaged in a fixed Ekman number simulation. An increase of the Rayleigh number indeed yields deviations (in terms of absolute correction) from the linear relation between P and Ra_Q^* . We conclude that in such configurations, the parameter range for which P is controlled is limited.

Keywords: Dynamo scaling laws; Numerical models for dynamo

1. Introduction

Power-based scaling laws introduced in Christensen and Aubert (2006) have been very successful in the dynamos community, and have been further developed in many recent studies (e.g. Jones 2011, Stelzer and Jackson 2013, Davidson 2013, Oruba and Dormy 2014). Davidson (2013) proposed a modified version of these original scaling laws, which is dedicated to planetary dynamos and which slightly differs from the original one because the non-linear inertial term is assumed to be negligible. Oruba and Dormy (2014) pointed out some “weaknesses” of the original scaling laws for the magnetic field strength. They stress that the power-based scaling laws essentially reflect the statistical balance between energy production and dissipation for saturated dynamos, and therefore work for any dynamo. Besides, these laws relate measured quantities (e.g. the magnetic field strength, or the flow strength) to another measured quantity, which is the power injected by buoyancy forces, as measured by the flux-based Rayleigh number Ra_Q^* (see (19) in Christensen and Aubert 2006).

The flux-based Rayleigh number Ra_Q^* involves the advected heat flow which is the difference between the time-averaged total heat flow and the conductive heat flow corresponding to the realized difference of temperature between both boundaries. There exists several contradictions and/or ambiguities in the literature concerning the nature of this parameter (controlled versus measured). Whereas there is a wide consensus on its measured nature in dynamos driven by an imposed difference of temperature between the boundaries, the literature is much less clear concerning its nature in the case of dynamos driven by an imposed heat flux. In Christensen (2010), it is suggested to be a control parameter in the context of heat flux

*Corresponding author. Email: ludivine.oruba@ens.fr

heating, whereas Aubert *et al.* (2009) refer to Ra_Q^* as being controlled only in the limit of vigorous enough convection. Finally, Dietrich *et al.* (2013) introduce Ra_Q^* as a control parameter, but the parameter they denote as Ra_Q^* corresponds to a slightly different definition from that of Christensen and Aubert (2006): it involves the heat flux at the outer boundary. With this definition, Ra_Q^* becomes a control parameter entering their governing equations.

The issue of the nature of the Ra_Q^* parameter is important, since this parameter is used to quantify the injected power involved in the power-based scaling laws. Such laws are then re-interpreted in the context of natural objects. The relation between Ra_Q^* and the injected power has first been highlighted by Christensen and Aubert (2006) in the particular context of convective dynamos, driven by an imposed difference of temperature between boundaries, in the spherical geometry with a linear radial profile of gravity. In this context, they stressed that for vigorous enough flows, the injected power is proportional to Ra_Q^* .

The configuration in Christensen and Aubert (2006) is however one among the numerous existing configurations in the literature on convective dynamos. Numerous mechanisms for driving convection have indeed been considered. Table 1 in Kutzner and Christensen (2002), for example, gathers a sample of the thermal or chemical boundary conditions implemented in numerical dynamos. Either the temperature, or the heat flux, can be fixed at one or both boundaries, and internal heating (or secular cooling) can also be implemented through a source (or sink) term in the temperature equation. Instead of the isothermal boundary conditions, these more complex configurations involving fixed heat flux can be used in an attempt to increase the relevance of numerical models to natural objects. They have been investigated in both purely convective studies (e.g. Gibbons *et al.* 2008), and in dynamo configurations, as in Sakuraba and Roberts (2009) and Hori *et al.* (2012).

Concerning the domain geometry, more attention has been paid to the spherical geometry because of its greater geophysical and astrophysical relevance. In this geometry, the radial profile of gravity commonly used by geophysicists corresponds to a uniform distribution of mass, and is therefore linear (e.g. Christensen *et al.* 2001), whereas studies motivated by giant planets and stars correspond to a central mass and have thus been performed with a gravity profile proportional to $1/r^2$ (e.g. Jones *et al.* 2011). In a purely hydrodynamical context, Gastine *et al.* (2015) tested the effect of various radial distributions of gravity on the boundary layer asymmetry. Nevertheless, the cartesian geometry is also interesting, as stressed by several recent studies (e.g. Stellmach and Hansen 2004, Tilgner 2014, Guervilly *et al.* 2015).

The issue of the robustness of the relation between the injected power and the Ra_Q^* parameter introduced by Christensen and Aubert (2006) is essential. It is important to understand to what extent such a relation can be used in numerical models and in planetary dynamos, and how it is modified by both the geometry and the driving mechanism. Gastine *et al.* (2015) shows analytically that the expression derived by Christensen and Aubert (2006) is valid (up to a geometrical factor) whatever the distance to the convection threshold for the particular choice of a gravity profile of the form $g \sim r^{-2}$. The case of fixed-flux boundary conditions has been examined by Aubert *et al.* (2009) in a study of the palaeo-evolution of the geodynamo. Their approach is based on the assumption that the total dissipation is proportional to the difference between the inner- and outer- boundary originated mass anomaly fluxes (see Buffett *et al.* 1996). This assumption however complicates the comparison with the analytical derivations of the type of Christensen and Aubert (2006).

The question of the nature (controlled versus measured) of Ra_Q^* , depending on the driving mechanism for convection clearly represents a gap in the literature. This paper aims at clarifying this issue, in a first part. The second objective of this paper is to further investigate the relation between the injected power and the flux-based Rayleigh number, in order to stress under which conditions the two quantities are proportional one to the other. The effect of the geometry and of the thermal heating mechanism is addressed. Our study is based on an analytical approach, supported by a database of numerical simulations.

2. Governing equations and control parameters

We study dynamos in the rotating thermal convection problem. The governing equations in the rotating reference frame under the Boussinesq approximation can be written in their non-dimensional form as

$$\partial_t \mathbf{u} + (\mathbf{u} \cdot \nabla) \mathbf{u} = -\nabla \pi + \text{Pr} \nabla^2 \mathbf{u} - 2 \frac{\text{Pr}}{\text{E}} \mathbf{e}_\Omega \times \mathbf{u} + \text{Ra Pr} \theta \mathbf{e}_g + (\nabla \times \mathbf{B}) \times \mathbf{B}, \quad (1)$$

$$\partial_t \mathbf{B} = \nabla \times (\mathbf{u} \times \mathbf{B}) + \frac{\text{Pr}}{\text{Pm}} \nabla^2 \mathbf{B}, \quad (2)$$

$$\partial_t \theta + (\mathbf{u} \cdot \nabla) (\theta + T_s) = \nabla^2 \theta, \quad (3)$$

$$\nabla \cdot \mathbf{u} = \nabla \cdot \mathbf{B} = 0, \quad (4)$$

where \mathbf{u} is the velocity field, \mathbf{B} the magnetic field and θ the deviation from the conductive temperature profile T_s . In the following, the total temperature will be denoted as T . The unit vectors \mathbf{e}_Ω and \mathbf{e}_g indicate the direction of the rotation axis and of gravity, respectively. They are defined such that $\boldsymbol{\Omega} = \Omega \mathbf{e}_\Omega$ and $\mathbf{g} = -g \mathbf{e}_g$.

The system (1–4) has been written by using d as unit of length, d^2/κ as unit of time and $\sqrt{\rho \mu \kappa}/d$ as unit of magnetic field. It yields the non-dimensional parameters $\text{E} = \nu/(\Omega d^2)$ (Ekman number), $\text{Pr} = \nu/\kappa$ (Prandtl number) and $\text{Pm} = \nu/\eta$ (magnetic Prandtl number), where ν is the kinematic viscosity of the fluid, $\kappa = k/(\rho c)$ is the thermal diffusivity, η is the magnetic diffusivity and Ω is the rotation rate. We introduce the Rayleigh number

$$\text{Ra} = \frac{\alpha g \Delta T^* d^3}{\nu \kappa}, \quad (5)$$

where α is the coefficient of thermal expansion, g the gravitational acceleration and ΔT^* the difference of temperature between both boundaries. Note that in case of an imposed flux boundary condition, the temperature must be averaged both in space (on the sphere) and in time in order to obtain a unique value for ΔT^* . Dimensional quantities are denoted with a star (*).

Our analysis will be tested against a wide database of 184 direct numerical simulations kindly provided by U. Christensen, corresponding to rigid boundaries. Most of them were previously reported in Christensen and Aubert (2006), Olson and Christensen (2006) and Christensen (2010). It covers the parameter range $\text{E} \in [10^{-6}, 10^{-3}]$, $\text{Pr} \in [10^{-1}, 10^2]$, $\text{Pm} \in [4 \times 10^{-2}, 66.70]$ and $\text{Ra} \in [10^5, 2.2 \times 10^9]$.

The nature (controlled versus measured) of parameters which measure the strength of convection depends on the thermal boundary conditions. For imposed temperature at both boundaries (differential heating, DH), the unit of temperature is ΔT^* , and the Rayleigh number Ra defined in (5) is a control parameter. Such is however not the case in configurations with fixed heat flux (fixed-flux heating, FF). In such configurations, either the heat flow Q^* is fixed at both boundaries, in which case the temperature is defined up to a constant, or Q^* is fixed at the outer boundary and the temperature is fixed at the inner boundary. For fixed-flux heating, a natural choice of unit of temperature is then $\varepsilon^2 Q^*/(\kappa \rho c d)$. It involves a factor ε related to the geometry of the domain (defined later in the text). It is convenient to define a modified Rayleigh number

$$\text{Ra}_\Phi = \frac{\alpha g \varepsilon^2 Q^* d^2}{\rho c \nu \kappa^2}, \quad (6)$$

where Q^* is the time-averaged heat flow across the layer (Joules per second). In fixed-flux heating, this parameter is indeed controlled, whereas the classical Rayleigh number is not.

The Nusselt number Nu allows to characterize the convective heat transport. It is defined as the ratio of the total time-averaged heat flux across the layer Q^* to the “purely diffusive” heat flow Q_{cond}^* , which corresponds to the heat flux which would be measured in the layer if the fluid was at rest with the realized ΔT^* . This last parameter corresponds to the difference between the temperature averaged in time and on both boundaries. Hence, $Q_{\text{cond}}^* = \varepsilon^{-2} \kappa \rho c d \Delta T^*$ and

$$Nu = \frac{Q^*}{\varepsilon^{-2} \kappa \rho c d \Delta T^*}, \quad (7)$$

that can be re-expressed as

$$Nu = \frac{Ra_\phi}{Ra}. \quad (8)$$

Besides, the quantity $Q_{\text{adv}}^* = Q^* - Q_{\text{cond}}^*$ is often used in the literature because independent on the vertical/radial coordinate (in the cartesian/spherical geometry). It allows to define the flux-based Rayleigh number as

$$Ra_Q^* = \frac{\alpha g Q_{\text{adv}}^* \varepsilon^2}{\rho c \Omega^3 d^4} = Ra(Nu - 1) \frac{E^3}{Pr^2} = (Ra_\phi - Ra) \frac{E^3}{Pr^2}. \quad (9)$$

The above expression can be re-expressed as

$$Ra_Q^* \frac{Nu}{Nu - 1} = \frac{Ra_\phi E^3}{Pr^2}. \quad (10)$$

In both differential and fixed-flux heating, Ra_Q^* is not a control parameter, since it involves both Ra and Ra_ϕ , which are respectively controlled, depending on the thermal boundary conditions. Nevertheless, according to (10), in the case of fixed-heat flux and if the convection is vigorous enough (i.e. $Nu \gg 1$), Ra_Q^* tends to a combination of control parameters $Ra_\phi E^3 / Pr^2$. The approximation $Nu \gg 1$ is very sensible for natural objects (stars or planets), but is not well justified for numerical dynamos (in present simulations, most dynamos operate at $Nu < 10$).

3. Relation between injected power and the flux-based Rayleigh number

The success of the Ra_Q^* parameter relies on its relation with the power injected by buoyancy forces, first derived in Christensen and Aubert (2006). The injected power P^* (in units Joule per second) in its dimensional form is

$$P^* = \iiint \rho \alpha g \theta^* \mathbf{e}_g \cdot \mathbf{u}^* dV^*, \quad (11)$$

which, in non-dimensional form (in units $\rho \kappa^3 d^{-1}$), becomes

$$\left[\frac{P^{\text{DH}}}{P^{\text{FF}}} \right] = \left[\frac{Ra Pr}{Ra_\phi Pr} \right] \iiint f_g \theta \mathbf{e}_g \cdot \mathbf{u} dV, \quad (12)$$

where f_g is a factor which depends on the geometry and on the radial profile of g . In the cartesian geometry with uniform gravity, $f_g = 1$. In the spherical geometry, the gravity g involved in the definitions (5) and (6) of Ra and Ra_ϕ corresponds to the value of gravity at r_o . This leads to $f_g = (r_o^2/d^2) r^{-2}$ for $g \sim r^{-2}$, and $f_g = (d/r_o) r$ for $g \sim r$. Note that in the above expressions, θ can equivalently be replaced by the total temperature T , because the integral over the volume of $(T_s \mathbf{e}_g \cdot \mathbf{u})$ vanishes.

This section aims at studying how the relation between the injected power and the Ra_Q^* parameter is affected by the geometry (cartesian versus spherical geometry, profile of gravity) and by the thermal boundary conditions (differential versus fixed-flux heating).

3.1. Expressions of heat flows in the cartesian and spherical geometries

In the cartesian configuration that is usually considered, the unit vectors \mathbf{e}_Ω and \mathbf{e}_g are parallel to the z -axis. The boundaries are separated by a distance d , and located at the planes $z = 0$ and $z = 1$. The horizontal coordinates are denoted as x and y , and vary between 0 and ε^{-1} , where $\varepsilon = d/L$ (L being the physical length of the domain in the x and y directions). The gravity is assumed to be uniform in the domain. The conductive temperature profile is solution of $\nabla^2 T_s = 0$. The choice of unit of temperature fixes dT_s/dz to unity, and the constant is chosen such that $T_s(0) = 1$, this leads to $T_s = 1 - z$.

The heat flow Q^* across the layer, which is independent on z , is the sum of the conductive heat flow Q_c^* and the advective heat flow Q_a^* , both of these being dependent on z . They are defined as

$$Q_c^*(z) = \kappa \rho c \iint -\nabla(T_s^* + \theta^*) \cdot \mathbf{e}_g dx^* dy^*, \quad Q_a^*(z) = \rho c \iint T^* u_z^* dx^* dy^*. \quad (13)$$

Using the above expression of T_s , the conductive heat flow becomes

$$\begin{bmatrix} Q_c^{*\text{DH}}(z) \\ Q_c^{*\text{FF}}(z) \end{bmatrix} = \begin{bmatrix} \kappa \rho c d \Delta T^* \\ \varepsilon^2 Q^* \end{bmatrix} \left(\varepsilon^{-2} - \iint \frac{\partial \theta}{\partial z} dx dy \right) \quad (14)$$

and the advective heat flow can be re-written as

$$\begin{bmatrix} Q_a^{*\text{DH}}(z) \\ Q_a^{*\text{FF}}(z) \end{bmatrix} = \begin{bmatrix} \kappa \rho c d \Delta T^* \\ \varepsilon^2 Q^* \end{bmatrix} \iint T u_z dx dy. \quad (15)$$

In the spherical configuration, the unit vector \mathbf{e}_g is radial, and is thus denoted as \mathbf{e}_r in following. The boundaries are spherical, and they are located between r_i and r_o (r_i and r_o are dimensional). In our study, the radial profile of gravity is assumed to be either linear, or proportional to $1/r^2$. The parameter d corresponds to the thickness of the shell $r_o - r_i$, and the geometrical factor ε is here defined as $\varepsilon^2 = d^2 / (4\pi r_o r_i) = (1 - \chi)^2 / (4\pi \chi)$, where $\chi = r_i / r_o$. Replacing ε^2 by its definition in (9) yields the expression introduced by Christensen and Aubert (2006)

$$\text{Ra}_Q^* = \frac{1}{4\pi r_o r_i} \frac{\alpha g Q_{\text{adv}}^*}{\rho c \Omega^3 d^2}. \quad (16)$$

Concerning the conductive temperature profile T_s , the choice of temperature units fixes $r^2 dT_s/dr = -\chi(1 - \chi)^{-2}$ and we chose the constant such that $T_s(r_i/d) = 1$. This yields $T_s = \chi(1 - \chi)^{-2} r^{-1} - \chi(1 - \chi)^{-1}$ and the corresponding dimensional expressions

$$T_s^{*\text{DH}} = \frac{\Delta T^* r_i r_o}{d} \frac{1}{r^*} + \left(1 - \Delta T^* \frac{r_o}{d} \right), \quad T_s^{*\text{FF}} = \frac{Q^*}{4\pi \kappa \rho c r^*} + \left(1 - \frac{Q^*}{4\pi \kappa \rho c r_i} \right). \quad (17)$$

Using (17) allows to re-express the conductive heat flow

$$Q_c^*(r) = \kappa \rho c \iint -\nabla(T_s^* + \theta^*) \cdot \mathbf{e}_r r^2 \sin \theta d\theta d\phi \quad (18)$$

as

$$\begin{bmatrix} Q_c^{*\text{DH}}(r) \\ Q_c^{*\text{FF}}(r) \end{bmatrix} = \begin{bmatrix} \kappa \rho c d \Delta T^* \\ \varepsilon^2 Q^* \end{bmatrix} \left(\varepsilon^{-2} - \iint \frac{\partial \theta}{\partial r} r^2 \sin \theta d\theta d\phi \right), \quad (19)$$

and the advective heat flow

$$Q_a^*(r) = \rho c \iint T^* u_r^* r^2 \sin \theta d\theta d\phi, \quad (20)$$

as

$$\begin{bmatrix} Q_a^{\text{DH}}(r) \\ Q_a^{\text{FF}}(r) \end{bmatrix} = \begin{bmatrix} \kappa \rho c d \Delta T^* \\ \varepsilon^2 Q^* \end{bmatrix} \iint T u_r r^2 \sin \theta \, d\theta \, d\phi. \quad (21)$$

The above expressions of the conductive and advective heat flows will be used to re-express the injected power (12) as a function of the Ra_Q^* parameter in the two next sections.

3.2. Differential heating

For differential heating, the Nusselt number defined in (7) can be re-expressed in the cartesian geometry, using (14a) and (15a) (Hereafter the labels “a” and “b” used on matrix equation references refer to the top and bottom row, respectively.), as

$$\text{Nu} = 1 - \varepsilon^2 \iint \frac{\partial \theta}{\partial z} \, dx \, dy + \varepsilon^2 \iint T u_z \, dx \, dy, \quad (22)$$

and in the spherical geometry, using (19a) and (21a), as

$$\text{Nu} = 1 - \varepsilon^2 \iint \frac{\partial \theta}{\partial r} r^2 \sin \theta \, d\theta \, d\phi + \varepsilon^2 \iint T u_r r^2 \sin \theta \, d\theta \, d\phi. \quad (23)$$

On time average and in the absence of internal sources or sinks of energy, the above expressions are independent on the radius r .

In the cartesian geometry, the expression (22) allows to rewrite the injected power (12a) as

$$P^{\text{DH}} = \text{RaPr} \int \left[\varepsilon^{-2} (\text{Nu} - 1) + \iint \frac{\partial \theta}{\partial z} \, dx \, dy \right] dz. \quad (24)$$

The integral in the second term vanishes because θ is zero at both boundaries, which leads to

$$P^{\text{DH}} = \left(\frac{\text{Pr}}{\text{E}} \right)^3 \text{Ra}_Q^* \varepsilon^{-2}. \quad (25)$$

In the spherical geometry with a radial profile of gravity of the form $g \sim r^{-2}$, the injected power (12a) can be re-expressed as

$$P^{\text{DH}} = \text{RaPr} \frac{r_o^2}{d^2} \iiint T \mathbf{e}_r \cdot \mathbf{u} \, dr \sin \theta \, d\theta \, d\phi. \quad (26)$$

Re-writing (26) as

$$P^{\text{DH}} = \text{RaPr} \frac{r_o^2}{d^2} \int \frac{1}{r^2} \left[\iint T u_r r^2 \sin \theta \, d\theta \, d\phi \right] dr, \quad (27)$$

allows to inject the expression (23) of the Nusselt number, which leads to

$$P^{\text{DH}} = \text{RaPr} \frac{r_o^2}{d^2} \int \frac{1}{r^2} \left[\varepsilon^{-2} (\text{Nu} - 1) + \iint \frac{\partial \theta}{\partial r} r^2 \sin \theta \, d\theta \, d\phi \right] dr. \quad (28)$$

The second term vanishes because of the boundary conditions, and we finally obtain

$$P^{\text{DH}} = \left(\frac{\text{Pr}}{\text{E}} \right)^3 \frac{4\pi}{(1 - \chi)^2} \text{Ra}_Q^*. \quad (29)$$

As expected, in the limit of a thin layer ($\chi \rightarrow 1$), this result tends to the cartesian result (25), since

$$\varepsilon^2 \left[\left(\frac{\text{Pr}}{\text{E}} \right)^3 \frac{4\pi}{(1 - \chi)^2} \text{Ra}_Q^* \right] \xrightarrow{\chi \rightarrow 1} \left(\frac{\text{Pr}}{\text{E}} \right)^3 \text{Ra}_Q^*. \quad (30)$$

The conclusions at this stage are that, for differential heating, there is an exact linear relation between the injected power and the Ra_Q^* parameter in the cartesian geometry, just like in the spherical geometry with a gravity profile proportional to $1/r^2$ (see also Gastine *et al.* 2015, for this last configuration). The proportionality factor however depends on the geometry.

Let us now focus on the geometry studied in Christensen and Aubert (2006), that is to say the spherical geometry with a linear radial profile of gravity. Here we aim at calculating the relation between the injected power and Ra_Q^* without any approximation. In this configuration, the convective power (12a) can be rewritten as

$$P^{\text{DH}} = \text{RaPr} \frac{d}{r_o} \iiint T \mathbf{e}_r \cdot \mathbf{u} r^3 dr \sin \theta d\theta d\phi. \quad (31)$$

Using expression (23) for the Nusselt number yields

$$P^{\text{DH}} = \text{RaPr} \frac{d}{r_o} \int r \left[\varepsilon^{-2} (\text{Nu} - 1) + \iint \frac{\partial \theta}{\partial r} r^2 \sin \theta d\theta d\phi \right] dr, \quad (32)$$

which can be re-expressed as

$$P^{\text{DH}} = 2\pi\chi \frac{1+\chi}{(1-\chi)^2} \left(\frac{\text{Pr}}{\text{E}} \right)^3 \text{Ra}_Q^* + \text{RaPr} (1-\chi) \iiint r^3 \frac{\partial \theta}{\partial r} dr \sin \theta d\theta d\phi. \quad (33)$$

Contrary to what happens in the cartesian geometry and in the spherical geometry with $g \sim r^{-2}$, the second term here involves an r^3 factor. This term therefore does not vanish. An integration by part leads to

$$P^{\text{DH}} = 2\pi\chi \frac{1+\chi}{(1-\chi)^2} \left(\frac{\text{Pr}}{\text{E}} \right)^3 \text{Ra}_Q^* - 3\text{RaPr} (1-\chi) \iiint \theta r^2 dr \sin \theta d\theta d\phi, \quad (34)$$

and that provides, after some rearrangements,

$$P^{\text{DH}} = \left(\frac{\text{Pr}}{\text{E}} \right)^3 \text{Ra}_Q^* \left[2\pi\chi \frac{1+\chi}{(1-\chi)^2} - 3(1-\chi) V \frac{\bar{\theta}}{\text{Nu} - 1} \right], \quad (35)$$

where the overbar indicates the mean over the volume of the shell, denoted as V . In the dimensional form, this yields

$$P^{\star\text{DH}} = (\rho\Omega^3 d^5) \text{Ra}_Q^* \left[2\pi\chi \frac{1+\chi}{(1-\chi)^2} - 3(1-\chi) V \frac{\bar{\theta}}{\text{Nu} - 1} \right]. \quad (36)$$

In this case, the relation between the injected power and Ra_Q^* is not purely linear. Relation (35) indeed exhibits an additional term in the square brackets, which corresponds to the relative correction from the linear relation between P and Ra_Q^* . It is proportional to the mean temperature perturbation over the shell, and stems from the assumption of a uniform distribution of mass in the spherical geometry. An estimation of this term can be made by estimating $\bar{\theta}$. We assume that in the boundary layers, the heat is purely transported by conduction. This hypothesis is combined to the assumption that the fluid is isothermal in the bulk (which is all the more verified that the convection is vigorous). The temperature in the bulk is denoted as T_m , and corresponds to the mean temperature over the shell \bar{T} , under the hypothesis of thin boundary layers. This yields

$$\left(\frac{r_i}{d} \right)^2 \frac{T_i - T_m}{\delta_i} \simeq \left(\frac{r_o}{d} \right)^2 \frac{T_m - T_o}{\delta_o}, \quad (37)$$

where δ_i and δ_o correspond to the thickness of the inner and outer boundary layers, respectively. A crude approach consists in assuming that the boundary layers are symmetric (i.e. $\delta_i = \delta_o$). The choice $T_i = 1$ and $T_o = 0$ leads to $T_m^{(a)} = \chi^2/(1+\chi^2)$, which

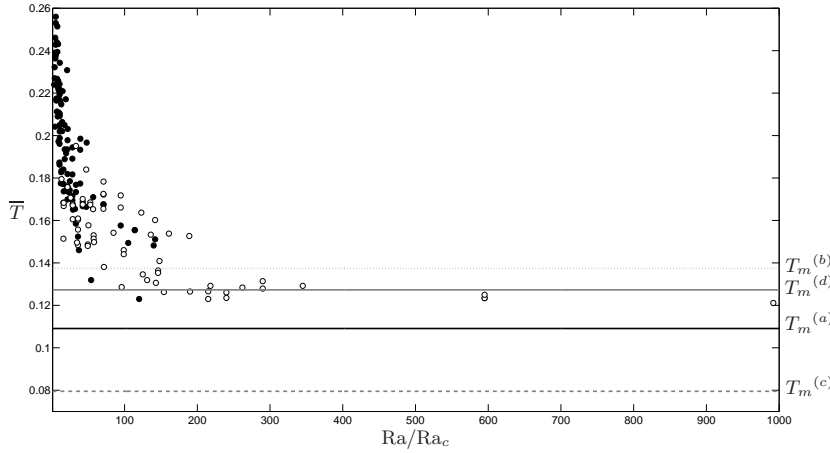


Figure 1. Representation of the mean temperature \bar{T} as a function of the Rayleigh number, normalized by the critical Rayleigh number at the threshold of convection. Points correspond to the full 184 dynamos database of U. Christensen. Bullets correspond to dipolar dynamos, circles to multipolar ones. Lines correspond to estimations of \bar{T} : $T_m^{(a)}$ (solid black), $T_m^{(b)}$ (dotted gray), $T_m^{(c)}$ (dashed gray) and $T_m^{(d)}$ (solid gray).

logically tends to $1/2$ as χ tends to unity. In the literature of convection in spherical geometry, alternative physical assumptions have been proposed to close the system (37) (e.g. Gastine *et al.* 2015). The assumption that thermal boundary layers are marginally stable (Vangelov and Jarvis 1994) provides, in this configuration, a value of the mean temperature in the bulk of $T_m^{(b)} = \chi^{7/4}/(1 + \chi^{7/4})$. The proposition by Wu and Libchaber (1991) that the thermal boundary layers adapt their temperature drops and their thicknesses such that their temperature scales $\nu\kappa/(g\alpha\delta^3)$ are equal yields $T_m^{(c)} = \chi^{7/3}/(1 + \chi^{7/3})$. Finally, very recently, Gastine *et al.* (2015) proposes that the inner and outer boundary layers exhibit the same density of plumes, which leads to $T_m^{(d)} = \chi^{11/6}/(1 + \chi^{11/6})$. These four estimates can be tested against the numerical database provided by U. Christensen, which corresponds to convective dynamos driven by differential heating and a linear radial profile of gravity. The aspect ratio is $\chi = 0.35$, which provides the estimates $T_m^{(a)} \simeq 0.1091$, $T_m^{(b)} \simeq 0.1374$, $T_m^{(c)} \simeq 0.0795$ and $T_m^{(d)} \simeq 0.1273$. Figure 1 shows the mean temperature in the shell as a function of the Rayleigh number, normalized by the critical Rayleigh number at the threshold of convection. Dynamos exhibiting a dipolar magnetic field are distinguished from multipolar dynamos. We observe that the mean temperature tends to a constant value, as the Rayleigh number increases. Both estimates $T_m^{(a)}$ and $T_m^{(d)}$ are remarkably well met by the multipolar dynamos associated to the most vigorous convection. We can notice that the simplest hypothesis (symmetric boundary layers) provides a very good agreement to the numerical database, which is not significantly improved by considering more elaborate assumptions.

Let us note that replacing \bar{T} by the estimated value $T_m^{(a)}$, and \bar{T}_s by

$$\bar{T}_s = \frac{\chi(-2\chi^2 + \chi + 1)}{2(1 - \chi^3)}, \quad (38)$$

in (35) yields

$$P^{\text{DH}} = \left(\frac{\text{Pr}}{\text{E}}\right)^3 \text{Ra}_Q^* \left[2\pi\chi \frac{1 + \chi}{(1 - \chi)^2} + \frac{2\pi f(\chi)}{\text{Nu} - 1} \right] \quad \text{with} \quad f(\chi) = \frac{\chi(1 + \chi)}{(1 + \chi^2)}, \quad (39)$$

and that in the limit $\chi \rightarrow 1$,

$$\varepsilon^2 P^{\text{DH}} \xrightarrow{\chi \rightarrow 1} \left(\frac{\text{Pr}}{\text{E}}\right)^3 \text{Ra}_Q^*, \quad (40)$$

which is consistent with the expression (25) derived in the cartesian geometry.

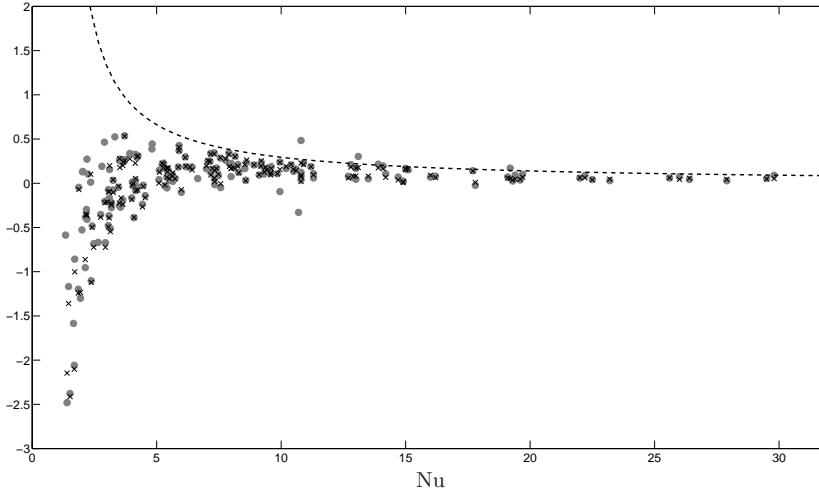


Figure 2. Representation of the relative correction term in (35), in the form $[P^{\text{DH}} - 2\pi\chi(1 + \chi)(1 - \chi)^{-2}\text{Ra}_Q^*]/\text{Ra}_Q^*$ (gray bullets) and $-3(1 - \chi)V\bar{\theta}(\text{Nu} - 1)^{-1}$ (black crosses) as a function of the Nusselt number Nu , using the numerical database provided by U. Christensen (P^{DH} is here in units $\rho\Omega^3 d^5$). The dashed line corresponds to the analytic function $f(\text{Nu}) = -3(1 - \chi)V(T_m^{(a)} - \bar{T}_s)(\text{Nu} - 1)^{-1}$; as expected, data tend asymptotically to this function for vigorous enough convection. This figure validates relation (35).

Figure 2 allows to test relation (35). It represents the relative correction term in (35), in the form

$$\frac{P^{\text{DH}} - 2\pi\chi(1 + \chi)(1 - \chi)^{-2}\text{Ra}_Q^*}{\text{Ra}_Q^*}$$

and

$$-3(1 - \chi)V\frac{\bar{\theta}}{\text{Nu} - 1},$$

using the present numerical database (P^{DH} is here in units $\rho\Omega^3 d^5$). The good agreement between both parts validates relation (35).

The first term on the right-hand side of (36) corresponds to the expression derived by Christensen and Aubert (2006). The second term, that we have just further investigated above, has been neglected in their study. This is equivalent to neglecting the contribution of the gradient of the temperature perturbation in the conductive heat flow (19a), compared to the gradient of the purely conductive profile T_s . Such an approximation is of course very sensible near the threshold of convection. At the threshold, this term indeed vanishes. In order to ponder on its reliability as convection becomes more vigorous, we represented in figure 3 the three terms of (36) in the form P^{DH} (in units $\rho\Omega^3 d^5$, gray bullets), $2\pi\chi(1 + \chi)(1 - \chi)^{-2}\text{Ra}_Q^*$ (black crosses) and the absolute correction term $-3(1 - \chi)V\bar{\theta}(\text{Nu} - 1)^{-1}\text{Ra}_Q^*$ (black circles), as a function of the flux-based Rayleigh number. The first panel corresponds to a log-log representation (as in Christensen and Aubert 2006), whereas the second one is linear. The figure based on logarithmic scales shows how the approximation consisting in neglecting the second term on the right-hand-side of (36) is sensible for the present database. Nevertheless, the linear representation indicates that in the numerical database, as the Ra_Q^* parameter becomes larger, this term increases. In planets and stars, however, $\text{Ra}_Q^* \ll 1$ and $\text{Nu} \gg 1$. For example, in the Earth's core, $\text{Ra}_Q^* \sim 10^{-13}$ and the Nusselt number based on the superadiabatic temperature gradient is about 10^6 (e.g. Olson and Christensen 2006, Christensen and Aubert 2006). This yields a negligible absolute correction term. The absolute correction term is also small in most existing numerical dynamos, with $\text{Ra}_Q^* \in [10^{-8}, 1]$ and $\text{Nu} \in [1, 32]$. The limit of the linear relation between the injected power and Ra_Q^* in this configuration, however, should not be

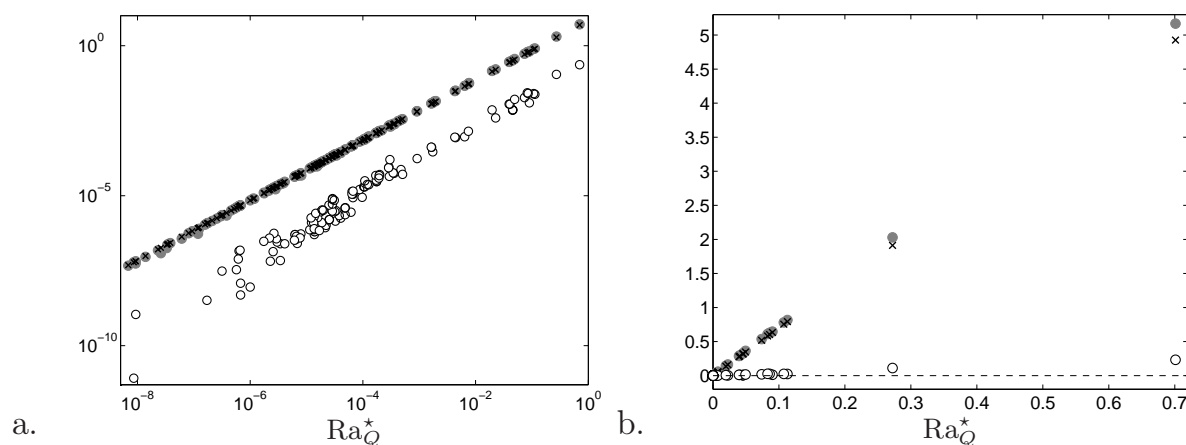


Figure 3. The three terms of (36) in the form P^{DH} (in units $\rho\Omega^3 d^5$, gray bullets), $2\pi\chi(1+\chi)(1-\chi)^{-2}\text{Ra}_Q^*$ (black crosses) and the absolute correction term $-3(1-\chi)V\bar{\theta}(\text{Nu}-1)^{-1}\text{Ra}_Q^*$ (black circles), as a function of the flux-based Rayleigh number, using the numerical database provided by U. Christensen. Panel (a) corresponds to a log-log representation, and panel (b) to a linear one.

ignored by numericists. Rewriting the absolute correction term as $-3(1-\chi)V\bar{\theta}\text{Ra}E^3/\text{Pr}^2$ using (9) reveals that trying to increase Nu (which is underestimated by a factor $\sim 10^5$ in existing simulations) through an increase of Ra at fixed E, will necessarily yield an increase of the correction term. However, as E can be decreased (with increasing computational resources), the Rayleigh number will have to increase as $\text{Ra}_c \sim E^{-4/3}$. For fixed super-criticality, the correction term will thus scale as $E^{5/3}$. Thus an increase in Ra/Ra_c can be achieved, while the correction term remains small. This is necessary to achieve a limit relevant to planetary cores.

This restriction neither exists in the spherical geometry with g proportional to $1/r^2$, nor in the cartesian geometry. As the original power-based scaling law for the magnetic field strength mainly reflects the statistical balance between injected power and dissipation (Oruba and Dormy 2014), our results allow to understand why the scaling law which relates the magnetic field strength to Ra_Q^* derived by Christensen and Aubert (2006) in the spherical geometry with $g \sim r$ is also verified in the planar convective-driven dynamos studied by Tilgner (2014) (see figure 1a therein). Besides, this highlighting of the role played by the gravity profile in the expression of the injected power corroborates the observation made by Raynaud *et al.* (2014) that the mass distribution has a strong influence on the fluid flow and thus on the dynamo generated magnetic field.

3.3. Fixed-flux at the CMB

We focus here on a configuration where the temperature is fixed at the inner boundary (ICB), which would correspond to the solidification temperature of iron at the pressure of the ICB, and the heat flux is fixed at the outer boundary (CMB), which is equivalent to considering that the mantle controls the heat flux out of the core.

The imposed heat flow Q^* is carried by the background temperature profile T_s . As a consequence, the Nusselt number reduces to $\text{Nu} = 1/\Delta T$, and the confrontation of the expressions of Q_c^{FF} and Q_a^{FF} in the cartesian geometry (see (14b) and (15b)) leads to

$$\iint \frac{\partial \theta}{\partial z} dx dy = \iint T u_z dx dy, \quad (41)$$

and (19b) and (21b) provide, in the spherical geometry,

$$\iint \frac{\partial \theta}{\partial r} r^2 \sin \theta \, d\theta \, d\phi = \iint T u_r r^2 \sin \theta \, d\theta \, d\phi. \quad (42)$$

In the cartesian geometry, (41) allows to rewrite the injected power (12b) as

$$P^{\text{FF}} = \text{Ra}_\phi \text{Pr} \int \left[\iint \frac{\partial \theta}{\partial z} \, dx \, dy \right] dz, \quad (43)$$

and replacing θ by $T - T_s$ provides

$$P^{\text{FF}} = \text{Ra}_\phi \text{Pr} \varepsilon^{-2} (-\Delta T + 1), \quad (44)$$

which can be rewritten as

$$P^{\text{FF}} = \left(\frac{\text{Pr}}{\text{E}} \right)^3 \text{Ra}_Q^* \varepsilon^{-2}. \quad (45)$$

This expression is thus identical to (25), derived in the differential heating configuration.

In the spherical geometry with $g \sim r^{-2}$, (42) allows to rewrite the injected power (27) as

$$P^{\text{FF}} = \text{Ra}_\phi \text{Pr} \frac{1}{(1-\chi)^2} \iiint \frac{\partial \theta}{\partial r} \, dr \, \sin \theta \, d\theta \, d\phi. \quad (46)$$

Introducing the notation $\langle \dots \rangle = 1/(4\pi) \iint \dots \sin \theta \, d\theta \, d\phi$ yields

$$P^{\text{FF}} = 4\pi \text{Ra}_\phi \text{Pr} \frac{1}{(1-\chi)^2} (\langle \theta \rangle_o - \langle \theta \rangle_i), \quad (47)$$

and replacing $\langle \theta \rangle$ by $\langle T \rangle - T_s$ leads to

$$P^{\text{FF}} = 4\pi \text{Ra}_\phi \text{Pr} \frac{1}{(1-\chi)^2} (-\Delta T + 1). \quad (48)$$

We finally obtain

$$P^{\text{FF}} = \left(\frac{\text{Pr}}{\text{E}} \right)^3 \frac{4\pi}{(1-\chi)^2} \text{Ra}_Q^*. \quad (49)$$

At this stage, the expressions (45) and (49) obtained for fixed-flux heating are thus the same as those derived in the differential heating configuration (see (25) and (29)).

In the spherical geometry with $g \sim r$, using (42) allows to rewrite the injected power (12b) as

$$P^{\text{FF}} = \text{Ra}_\phi \text{Pr} \frac{d}{r_o} \iiint \frac{\partial \theta}{\partial r} r^3 \, dr \, \sin \theta \, d\theta \, d\phi, \quad (50)$$

which becomes, after an integration by part

$$P^{\text{FF}} = 4\pi \text{Ra}_\phi \text{Pr} \frac{d}{r_o} \left[\left[\langle \theta \rangle r^3 \right]_{r_i/d}^{r_o/d} - 3 \int r^2 \langle \theta \rangle \, dr \right]. \quad (51)$$

As the temperature at the inner boundary is imposed ($\theta_i = 0$), we obtain

$$P^{\text{FF}} = 4\pi \text{Ra}_\phi \text{Pr} \frac{d}{r_o} \left[\frac{\langle \theta \rangle_o}{(1-\chi)^3} - 3 \int r^2 \langle \theta \rangle \, dr \right], \quad (52)$$

and replacing $\langle \theta \rangle_o$ by $\langle T \rangle_o - \langle T \rangle_i + T_i - T_o$ yields

$$P^{\text{FF}} = 4\pi \text{Ra}_\phi \text{Pr} \frac{d}{r_o} \left[\frac{1}{(1-\chi)^3} (-\Delta T + 1) - 3 \int r^2 \langle \theta \rangle \, dr \right], \quad (53)$$

and finally

$$P^{\text{FF}} = \left(\frac{\text{Pr}}{\text{E}}\right)^3 \text{Ra}_Q^* \left[\frac{4\pi}{(1-\chi)^2} - 3(1-\chi)V \frac{\text{Nu}}{\text{Nu}-1} \bar{\theta} \right]. \quad (54)$$

It is interesting to note that as for differential heating, this geometry exhibits a supplementary term involving the mean perturbation temperature. The correction terms in (35) and (54) differ through a Nu factor, which corresponds to the ratio of the two factors in (12a,b). In the limit of vigorous convection, $\bar{\theta}^{\text{DH}}$ is $O(1)$ whereas $\bar{\theta}^{\text{FF}}$ is approximately proportional to $1/\text{Nu}$. The correction terms in (35) and (54) thus tend to a unique expression, which is consistent with the idea that when convection is very vigorous, the effect of different thermal boundary conditions vanishes (e.g. Johnston and Doering 2009). The same restriction for the linear relation between the injected power and the flux-based Rayleigh number thus also applies to the fixed-flux configuration.

3.4. Chemical convection with fixed flux at the ICB

The most general cases can involve internal volumetric sources or sinks of energy. Let us focus on the configuration of an imposed uniform heat flux Q_i^* at the ICB, zero flux at the CMB and homogeneous volumetric sinks (to mimic chemical convection with fixed flux at the ICB, as introduced in Kutzner and Christensen 2002). The sink term provides a modification of the conductive temperature profile T_s , so that the heat equation (3) remains unchanged. In this case, the unit of temperature $\mathcal{C}\varepsilon^2 Q_i^*/(\kappa\rho cd)$, with $\mathcal{C} = (2+\chi)/(2(1+\chi+\chi^2))$ a geometric factor, is chosen such that $\Delta T_s = 1$. This yields

$$T_s = \frac{\chi}{2+\chi} \left[\frac{-3}{(1-\chi)^2} + r^2 + \frac{2}{r(1-\chi)^3} \right], \quad (55)$$

where $T_s(r_i/d)$ has been set to unity. As the time-averaged total heat flow Q^* here depends on radius, the Nusselt number defined in (7) also depends on radius. We therefore define a reference Nusselt number Nu^\dagger as

$$\text{Nu}^\dagger = \frac{\Delta T_s^*}{\Delta T^*} = \frac{1}{\Delta T^*}. \quad (56)$$

Now, introducing

$$\text{Ra}_\Phi^\dagger = \frac{\alpha g \varepsilon^2 \mathcal{C} Q_i^* d^2}{\rho c \nu \kappa^2}, \quad (57)$$

yields $\text{Nu}^\dagger = \text{Ra}_\Phi^\dagger / \text{Ra}$. Note that as χ tends to unity, \mathcal{C} tends to $1/2$. In this limit, the comparison of Ra_Φ and Ra_Φ^\dagger relies on the substitution of the time-averaged total heat flow Q^* (which is a constant in the absence of energy sink) by its volume average (equal to $Q_i^*/2$) in the presence of energy sink. Because of the homogeneous Neumann boundary conditions, the temperature perturbation is defined up to an arbitrary constant. If this constant is chosen such that $\langle \theta \rangle_i = 0$, the expressions (49) and (54) for the injected power, derived in the configuration of fixed-flux heating with no volumetric source, are recovered in the presence of a sink of energy, provided Ra_Q^* is replaced by

$$(\text{Ra}_\Phi^\dagger - \text{Ra}) \frac{\text{E}^3}{\text{Pr}^2} = \frac{\alpha g \kappa (\Delta T_s^* - \Delta T^*)}{\Omega^3 d^3}. \quad (58)$$

The conclusions are thus identical to those derived in the case of no internal energy sources/sinks.

4. Conclusions

In this paper, we first focused on the Ra_Q^* parameter which plays an essential role in the power-based scaling laws in dynamo. We highlighted that for vigorous enough convection (i.e. $Nu \gg 1$), the Ra_Q^* parameter tends to a combination of parameters which are controlled in the case of fixed-heat flux. However sensible for natural objects, this approximation is not straightforward for numerical dynamos in present databases. This clarifies the contradictions in the literature concerning the nature (controlled versus measured) of this parameter in convective dynamos driven by a fixed-heat flux.

In a second part, we investigated the issue of the robustness of the original relation between the power P injected by buoyancy forces and the Ra_Q^* parameter with the geometry and the thermal heating mechanism. This is an important question since this robustness is mandatory for the extrapolations of the original power-based scaling laws to other configurations to be relevant. We have shown analytically that in the cartesian geometry as in the spherical geometry exhibiting a radial profile of gravity of the form $1/r^2$, for both differential and fixed-flux heating, the linear relation between the injected power and Ra_Q^* is robust. Only the proportionality factor is modified by the geometry. The spherical geometry with a linear radial profile of gravity is however more complicated, since the relation between P and Ra_Q^* involves an additional term proportional to the mean perturbation temperature. In the differential heating configuration, we have highlighted and pondered on this term by using a numerical database of dynamos. We have shown that it could be estimated in the limit of vigorous convection through simple assumptions. We have also stressed that the linear approximation between P and Ra_Q^* is relevant to natural dynamos and in most existing numerical dynamos.

Its validity however places an upper-bound on the strength of the driving which can be envisaged in a fixed Ekman number simulation. An increase of the Rayleigh number indeed yields deviations (in terms of absolute correction) from the linear relation between P and Ra_Q^* . The effect of the heating mode on the relation between P and Ra_Q^* is found to be small.

To summarize, in convective dynamos driven by a fixed-heat flux, the Ra_Q^* parameter becomes controlled provided the Nusselt number is large enough ($Nu \gg 1$). However, in the geometry commonly studied by geophysicists (spherical with uniform mass distribution), an increase of the Rayleigh number in numerical simulations at fixed Ekman number would yield a deviation of P from Ra_Q^* . The parameter range for which the power injected by buoyancy forces is controlled is thus limited. In the quest for predictive scaling laws, an alternative approach to power-based scaling laws consists in expressing forces balances based on the distance to the onset of dynamo action (see Petrelis and Fauve 2001, Oruba and Dormy 2014).

Acknowledgments

The author wants gratefully thank Uli Christensen for sharing his numerical database, and Emmanuel Dormy for useful discussions.

References

- Aubert, J., Labrosse, S. and Poitou, C., Modelling the palaeo-evolution of the geodynamo. *Geophys. J. Int.*, 2009, **179**, 1414-1428.
- Buffett, B.A., Huppert, H., Lister, J. and Woods, A., On the thermal evolution of the Earth's core. *J. geophys. Res.*, 1996, **101**(B4), 7989-8006.
- Christensen, U., Dynamo Scaling Laws and Applications to the Planets. *Space Sci. Rev.*, 2010, **152**, 565-590.
- Christensen, U. and Aubert, J., Scaling properties of convection-driven dynamos in rotating spherical shells and application to planetary magnetic fields. *Geophys. J. Int.*, 2006, **166**, 97-114.
- Christensen, U., Aubert, J., Cardin, P., Dormy, E., Gibbons, S., Glatzmaier, G., Grote, E., Honkura, Y.,

- Jones, C., Konoh, M., Matsushima, M., Sakuraba, A., Takahashi, F., Tilgner, A., Wicht, J. and Zhang, K., A numerical dynamo benchmark. *Phys. Earth Planet. Int.*, 2001, **128**, 25–34.
- Davidson, P., Scaling laws for planetary dynamos. *Geophys. J. Int.*, 2013, **195**, 67–74.
- Dietrich, W., Schmitt, D. and Wicht, J., Hemispherical Parker waves driven by thermal shear in planetary dynamos. *Europhys. Lett.*, 2013, **104**.
- Gastine, T., Wicht, J. and Aurnou, J.M., Turbulent Rayleigh-Benard convection in spherical shells. *J. Fluid. Mech.*, 2015, **778**, 721–764.
- Gibbons, S., Gubbins, D. and Zhang, K., Convection in rotating spherical fluid shells with inhomogeneous heat flux at the outer boundary. *Geophys. Astrophys. Fluid Dyn.*, 2008, **101:5**, 347–370.
- Guervilly, C., Hughes, D.W. and Jones, C.A., Generation of magnetic fields by large-scale vortices in rotating convection. *Phys. Rev. E*, 2015, **91**, 041001.
- Hori, K., Wicht, J. and Christensen, U., The influence of thermo-compositional boundary conditions on convection and dynamos in a rotating spherical shell. *Phys. Earth Planet. Int.*, 2012, **196-197**, 32–48.
- Johnston, H. and Doering, C., Comparison of turbulent thermal convection between conditions of constant temperature and constant flux. *Phys. Rev. Lett.*, 2009, **102**, 064501.
- Jones, C.A., Planetary magnetic fields and fluid dynamos. *Annu. Rev. Fluid Mech.*, 2011, **43**, 583614.
- Jones, C., Boronski, P., Brun, A., Glatzmaier, G., Gastine, T., Miesch, M. and Wicht, J., Anelastic convection-driven dynamo benchmarks. *Icarus*, 2011, **216**, 120–135.
- Kutzner, C. and Christensen, U., From stable dipolar towards reversing numerical dynamos. *Phys. Earth Planet. Int.*, 2002, **131**, 29–45.
- Olson, P. and Christensen, U.C., Dipole moment scaling for convection-driven planetary dynamos. *Earth Planet. Sci. Lett.*, 2006, **250**, 561–571.
- Oruba, L. and Dormy, E., Predictive scaling laws for spherical rotating dynamos. *Geophys. J. Int.*, 2014, **198**, 828–847.
- Petrelis, F. and Fauve, S., Saturation of the magnetic field above the dynamo threshold. *Eur. Phys. J. B*, 2001, **22**, 273–276.
- Raynaud, R., Petitdemange, L. and Dormy, E., Influence of the mass distribution on the magnetic field topology. *Astron. Astrophys.*, 2014, **567**, A107.
- Sakuraba, A. and Roberts, P., Generation of a strong magnetic field using uniform heat flux at the surface of the core. *Nature Geoscience*, 2009, **2**, 802–805.
- Stellmach, S. and Hansen, U., Cartesian convection driven dynamos at low Ekman number. *Phys. Rev.*, 2004, **70**, 056312.
- Stelzer, Z. and Jackson, A., Extracting scaling laws from numerical dynamo models. *Geophys. J. Int.*, 2013, **193**, 1265–1276.
- Tilgner, A., Magnetic energy dissipation and mean magnetic field generation in planar convection-driven dynamos. *Phys. Rev.*, 2014, **90(1)**, 013004.
- Vangelov, V.I. and Jarvis, G.T., Geometrical effects of curvature in axisymmetric spherical models of mantle convection. *J. Geophys. Res.*, 1994, **99**, 9345–9358.
- Wu, X.Z. and Libchaber, A., Non-Boussinesq effects in free thermal convection. *Phys. Rev.*, 1991, **43**, 2833–2839.